EOSC 579 - Chapter 2 - Internal Waves. Lecture 3: Moving in a Nonuniform Environment

3.1 Learning Goals

As the end of this lecture you will be able to:

- Describe how internal waves change as they propagate into a region of stronger (or weaker) stratification
- Describe how internal waves are generated as lee waves
- Describe how internal waves break

3.2 Speeds

It is useful to have the full equations for the phase velocity and group velocity.

$$\vec{c}_{\text{phase}} = \frac{(N^2k^2 + f^2m^2)^{1/2}}{(k^2+m^2)^{3/2}}(k, m) \tag{1}$$

(2)

$$\vec{c}_{\text{group}} = \left(N^2 - f^2\right) \frac{mk}{\omega(k^2+m^2)^2}\,(m, -k) \tag{3}$$

3.3 Changing N

The dispersion relation for internal waves is:

$$\tan^2\theta = \frac{\omega^2 - f^2}{N^2 - \omega^2} \tag{4}$$

and

$$\tan\theta = \frac{k}{m} \tag{5}$$

Thus if an internal wave propagates into a region of higher stratification (N increases)

- θ decreases, k/m decreases, the wave phase propagation becomes more vertical
- As k cannot change at horizontal changes, the vertical wave number m increases

- As the wave phase velocity becomes more vertical, the group velocity becomes more horizontal

Generally ocean stratification decreases with depth, so wave beams (or rays) are more horizontal near the surface and become more vertical at depth.

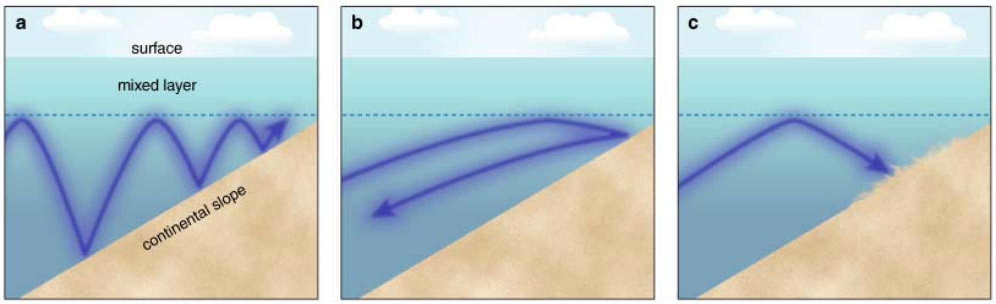

Figure 3.1: *Wave beams approaching a shore in a typical, strong stratification near surface, case. Barbara Aulicion as shown in Cacchione and Pratson 2004.*[1]

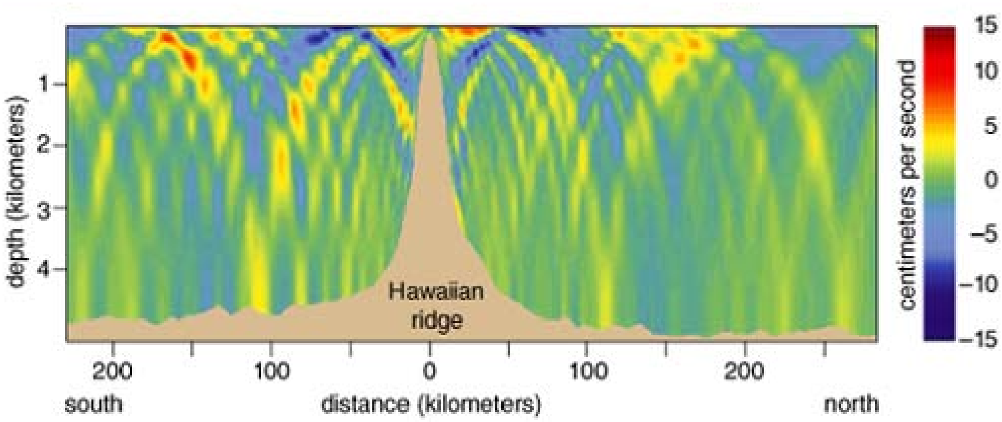

Figure 3.2: *Numerical model results showing wave beams generated at the Hawaiian Ridge. Holloway and Merrifield 2003 as shown in Cacchione and Pratson 2004.*[1]*.*

If internal waves propagate toward a region where N is lower than their ω, they will reflect. The group velocity will become vertical and slower. In the region where N is lower than ω, the wave cannot propagate. It will be evanescent, decaying away from the reflection.

3.4 Internal, Lee, Wave Generation over Corrugations

We discussed how internal waves can be generated where tidal flow goes over topography that is at the critical slope for that frequency. That is where the angle of the topography

[1] `https://www.americanscientist.org/article/internal-tides-and-the-continental-slope`

satisfies

$$\tan^2 \theta = \frac{\omega^2 - f^2}{N^2 - \omega^2} \tag{6}$$

A tractable and illuminating example of internal wave generation is to consider a steady flow over a sinusoidal topography. Following Cushman-Roisin 1994, we consider the analogous case of a fluid at rest, with a sinusoidal topography moving at a steady rate $-U$ below it (Figure 3.3)

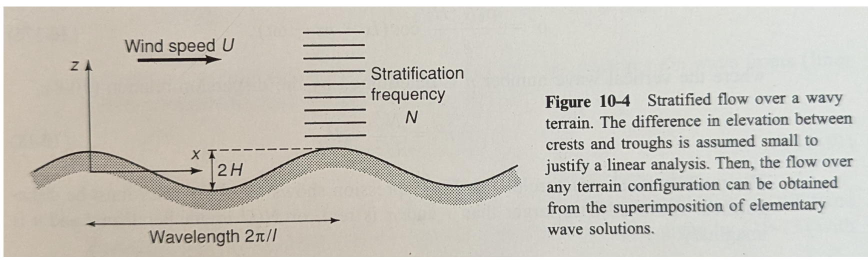

Figure 3.3: *Set up for waves above a moving, corrugated surface. From Cushman-Roisin 1992. Note he uses ℓ for $-\kappa$.*

So if the topography is given by $h = H \cos \kappa x$, it will generate oscillations at its wavenumber κ and a frequency $\omega = |\kappa| U$ The bottom will move as:

$$z = h(x + Ut) = H \cos [\kappa(x + Ut)] \tag{7}$$

$$= H \cos [-\kappa x - \omega t] \tag{8}$$

Note that as our convention is for ω to be positive, our wavenumber is negative $-\kappa$.

The basic boundary condition, no flow through the bottom, means that the vertical and horizontal velocity at the bottom must linked through:

$$w = \frac{\partial h}{\partial t} + u \frac{\partial h}{\partial x} \tag{9}$$

at $z = h$. Assuming small topography (so we can have small, linear, waves), h is small and

u is small, we get the linear version (at $z = 0$ the bottom)

$$w = \frac{\partial h}{\partial t} \tag{10}$$

$$= H\omega \sin(-\kappa x - \omega t) \tag{11}$$

Then we can find an internal wave solution that satisfies this bottom boundary condition:

$$w = \kappa U H \sin(-\kappa x + mz - \omega t) \tag{12}$$

$$u = mUH \sin(-\kappa x + mz - \omega t) \tag{13}$$

$$p' = -\rho_o m U^2 H \sin(-\kappa x + mz - \omega t) \tag{14}$$

$$\rho' = \frac{\rho_o N^2 H}{g} \cos(-\kappa x + mz - \omega t) \tag{15}$$

$$\tag{16}$$

The angle of the wave vector is set by the frequency and thus, ignoring f, the vertical wave number is given by

$$m^2 = \frac{N^2}{U^2} - \kappa^2 \tag{17}$$

There are two choices. If N/U is larger than $|\kappa|$, then the vertical wavenumber is real and we have propagating waves. if N/U is smaller than $|\kappa|$ then we have trapped waves, or waves decaying in the vertical from the boundary.

Propagating Case

$$m = \pm \left(\frac{N^2}{U^2} - \kappa^2 \right)^{1/2} \tag{18}$$

where we must chose $m < 0$ so that the group velocity is upwards, away from the boundary. Our k is negative, thus the phase velocity is down and to the left, meaning our group velocity is up and to the left (relative group velocity in Figure 3.4). That is the group velocity is away from the boundary and propagating in the direction the bottom is moving.

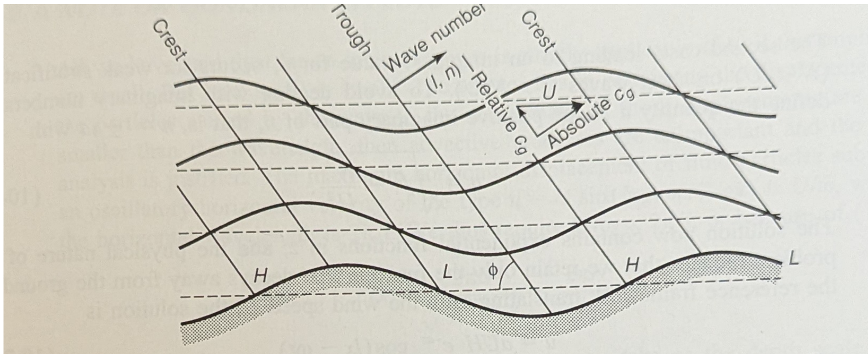

Figure 10-5 Structure of the mountain wave in the case of strong stratification or long wavelength ($N > lU$). Note the absence of vertical attenuation and the presence of a phase shift with height. The group velocity with respect to the ground is oriented upward and downwind. The pressure distribution, with highs on wind-facing slopes and lows on flanks in the wind's shadow, exerts a drag on the moving air mass.

Figure 3.4: *Result for propagating waves. From Cushman-Roisin 1992. Note he uses ℓ for $-\kappa$ and n for m.*

Trapped Case In this case we find the vertical wave number is imaginary.

$$m = \pm ia = \pm i \left(\kappa^2 - \frac{N^2}{U^2} \right)^{1/2} \tag{19}$$

and we need to chose the sign of m to give us decreasing exponentials away from the ground. Thus

$$\begin{aligned} w &= \kappa U H \exp(-az) \sin(-kappax - \omega t) && (20) \\ u &= aUH \exp(-az) \cos(-kappax - \omega t) && (21) \\ p' &= -\rho_o a U^2 H \exp(-az) \cos(-kappax - \omega t) && (22) \\ \rho' &= \frac{\rho_o N^2 H}{g} \exp(-az) \cos(-kappax - \omega t) && (23) \\ & && (24) \end{aligned}$$

The solution is locked to the topography, with no phase propagation with height. The waves "damp" as we more upwards (Figure 3.5)

3.5 Breaking Internal Waves

Based on notes originally written by Stephanie Waterman.

In the stratified ocean interior, turbulent mixing is most often generated by the breaking

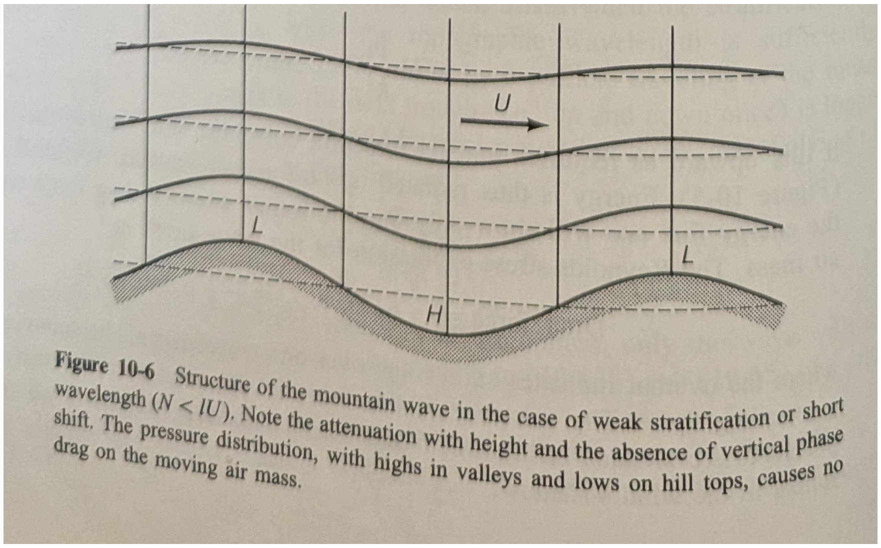

Figure 3.5: *Result for trapped waves. From Cushman-Roisin 1992.*

of internal waves. Internal waves do not break at their"crests" but rather where the shear is largest. That is internal waves break by shear instabilities.

Low frequency, long period, near-inertial internal wave motions have relatively small vertical wavelengths of 10-100 m in the open ocean (and only 1-10 m in shallow seas). These small length scales cause the currents associated with the wave motion to vary rapidly in the vertical, creating large vertical shear.

Instability can result if the shear becomes large. When internal wave shear becomes large enough to overcome the stabilizing effect of the density stratification, it generates a primary instability that we call the Kelvin-Helmholtz (KH) type. The tendency for this instability to grow despite the damping action of stable stratification is quantified using a non-dimensional number (the so-called *gradient Richardson number*, Ri,) given by the ratio of the squared buoyancy frequency N (a measure of the strength of the density stratification) to the squared vertical shear of the horizontal flow. When the internal wave shear is strong enough (or stratification weak enough) to bring Ri below a critical value, instability is possible.

Visual evidence for KH instability frequently can be seen at the top of the atmospheric boundary layer in late afternoon and evening, where it appears as patches of banded clouds (Figure 3.6c). Seen from the side, such clouds often take shapes similar to those of surface waves breaking on a beach (Figure 3.6a and b). A daring scientific diver also took photos

Figure 3.6: *Kelvin-Helmholtz billows revealed by clouds. (a) Side view (from www-frd.fsl.noaa.gov/mab/scatcat; photo by Brooks Martner). (b) Kelvin- Helmholtz billows made visible by a fog layer on the shore of Nares Strait in the Canadian arctic (courtesy of Scott McAuliffe, Oregon State University). (c) Ground view of billow clouds (www.weathervortex.com/sky-ribbons.htm), showing large-scale knot instabilities (Thorpe, 2002) and thin striations consistent with convection rolls (Klaassen and Peltier, 1991).*

of dye streaks which show clear observations of the presence and structure of KH billows in the ocean (Figure 3.7).

The "roll-up" of so-called KH billows (formed by the primary instability) (see Figure 3.8 for a nice image of this in the lab) is only the first step: the shear of the billows leads to a secondary instability which forms and destroys the billow structures. Eventually the flow develops into so-called fully-developed 3-dimensional turbulence (Figure 3.9), and the wave has "broken".

The shear layer of the wave (Figure 3.9 upper left) 'rolls up' due to the K-H instability (Figure 3.9 upper right). The K-H instability leads to density overturns, which cause mixing (Figure 3.9 middle) leading to turbulence and a thickening of the shear layer and density gradient (Figure 3.9 lower).

We are still learning about the internal wave breaking process and its implications for the ocean's mixing rate: the topic is currently an area of active research. We pursue this research with very high resolution numerical simulations of wave breaking (*e.g.* Figure 3.9). Recently, increasingly specialized, ultra-high resolution observations of the ocean also give us a view of wave breaking in the real world (see Figures 3.10 and 3.11).

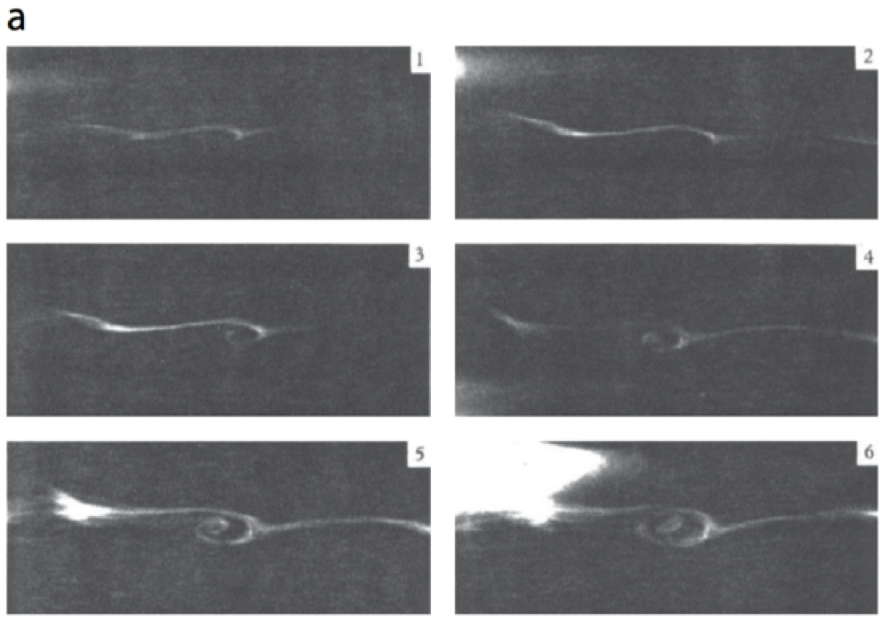

Figure 3.7: *Underwater snapshots made by divers from laboriously executed dye release experiments in the Mediterranean thermocline. From: Woods, J.D. 1968. Wave-induced shear instability in the summer thermocline. Journal of Fluid Mechanics 32: 791-800.*

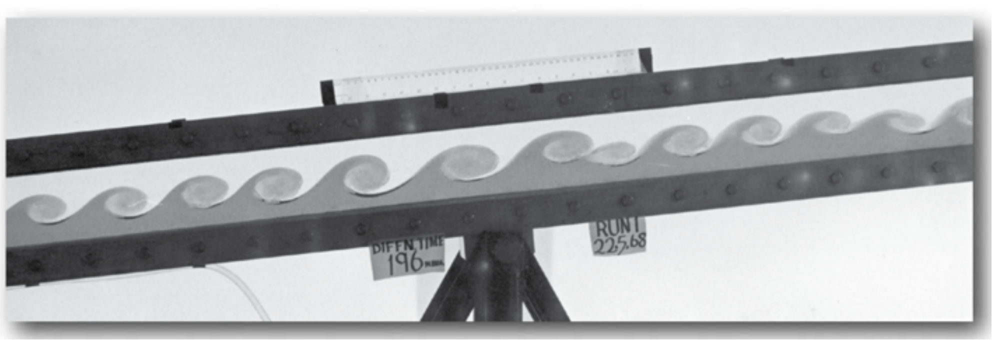

Figure 3.8: *Tilting tank laboratory experiment in which a dense (here, dark) layer of fluid underlies a lighter fluid initially at rest. When the tank is tilted, buoyant forces accelerate the denser fluid down and the lighter fluid up the slope, thereby creating a velocity gradient across the interface and subsequent billow formation. From: Thorpe, S.A. 1971. Experiments on the instability of stratified shear flows: Miscible fluids. Journal of Fluid Mechanics 46: 299 - 319.*

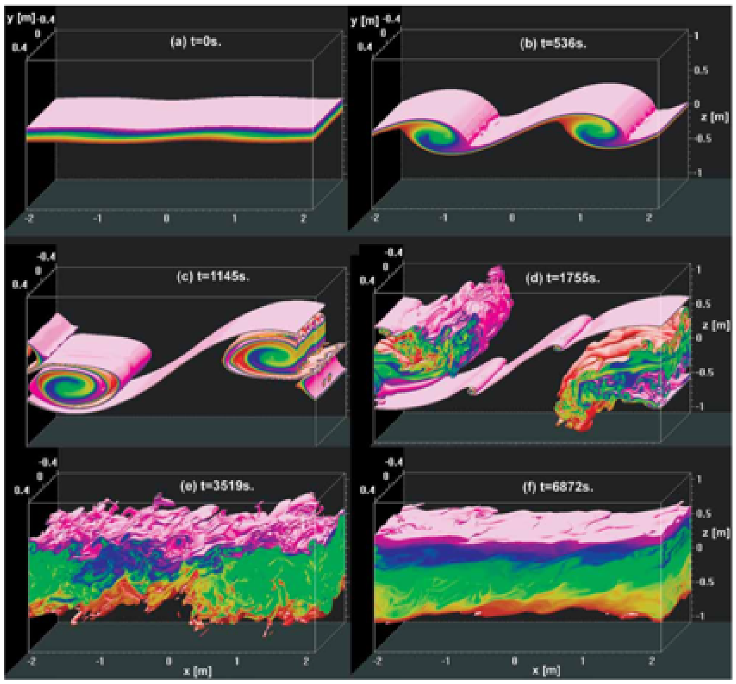

Figure 3.9: *Direct numerical simulations of the density field at successive times in the life cycle of a Kelvin-Helmholtz billow train. Colours show density in the transition layer; upper and lower homogeneous layers are rendered transparent. (a) The initial state is a two-layer flow, with a lower (dense) layer flowing to the left and an upper layer to the right. a small perturbation is applied. (b) Two wavelengths of the primary Kelvin-Helmholtz instability. (c) Kelvin-Helmholtz billows are beginning to pair. Secondary instability is visible in a cutaway at upper right, taking the form of shear-aligned convection rolls. (d) Secondary shear instability forms on the braids. (e) The fully turbulent state. (f) Turbulence decays to form sharp layers and random small-scale waves. From: Smyth, W.D., and J.N. Moum. 2012. Ocean mixing by Kelvin-Helmholtz instability. Oceanography 25(2): 140-149.*

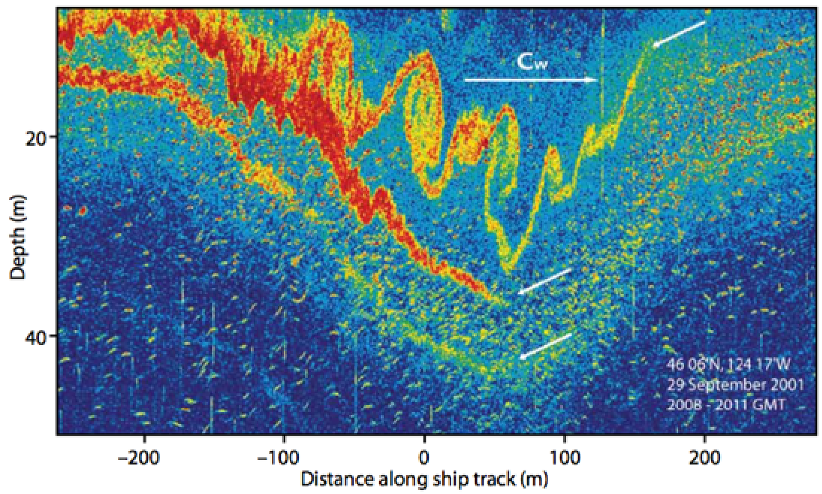

Figure 3.10: *Example acoustical snapshot of a nonlinear internal gravity wave approaching the Oregon coast. The wave propagates from left to right at speed Cw in this image. The velocity in the upper layer is in the direction of Cw, and the resultant current shear defines the direction of the rollups in the billows. The bright acoustic scattering layers result from reflections by density microstructure caused by turbulence. The signal reveals a train of Kelvin-Helmholtz billows. From: Mashayek, A., and W.R. Peltier. 2011. Shear-induced mixing in geophysical flows: does the route to turbulence matter to its efficiency? J. of Fluid Mech. 725: 216-261.*

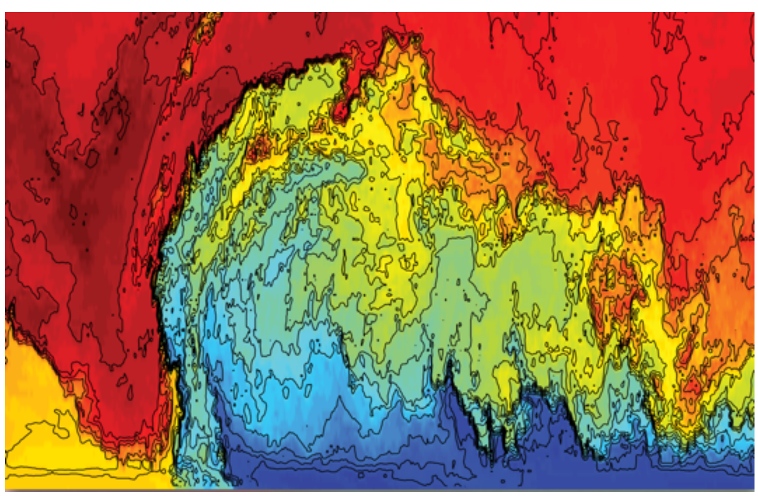

Figure 3.11: *A large backward-breaking internal wave is depicted in this time-depth image whose axes are 14 minutes horizontally and 50 m vertically. This wave was observed using 101 high-sampling rate temperature sensors between 0.5 and 50 m above the bottom at 550 m depth near the top of Great Meteor seamount in the North Atlantic Ocean. Temperature ranges from 12.3^{o}C (blue) to 14.1^{o}C (red). Contour intervals are every 0.1^{o}C (black). From: van Haren, H., and L. Gostiaux. 2012. Energy release through internal wave breaking. Oceanography 25(2):124-131.*